



Removal of cobalt ions from aqueous solutions by polymer assisted ultrafiltration using experimental design approach. part 1: Optimization of complexation conditions

Corneliu Cojocaru^{*,1}, Grażyna Zakrzewska-Trznadel, Agnieszka Jaworska

Department of Nuclear Methods in Process Engineering, Institute of Nuclear Chemistry and Technology, Dorodna 16, 03-195 Warsaw, Poland

ARTICLE INFO

Article history:

Received 5 November 2008

Received in revised form 14 February 2009

Accepted 30 March 2009

Available online 7 April 2009

Keywords:

Polymer assisted ultrafiltration

Complexation

Heavy metal removal

Response surface methodology

ABSTRACT

The polymer assisted ultrafiltration process combines the selectivity of the chelating agent with the filtration ability of the membrane acting in synergy. Such hybrid process (complexation–ultrafiltration) is influenced by several factors and therefore the application of experimental design for process optimization using a reduced number of experiments is of great importance.

The present work deals with the investigation and optimization of cobalt ions removal from aqueous solutions by polymer enhanced ultrafiltration using experimental design and response surface methodological approach. Polyethyleneimine has been used as chelating agent for cobalt complexation and the ultrafiltration experiments were carried out in dead-end operating mode using a flat-sheet membrane made from regenerated cellulose. The aim of this part of experiments was to find optimal conditions for cobalt complexation, i.e. the influence of initial concentration of cobalt in feed solution, polymer/metal ratio and pH of feed solution, on the rejection efficiency and binding capacity of the polymer. In this respect, the central compositional design has been used for planning the experiments and for construction of second-order response surface models applicable for predictions. The analysis of variance has been employed for statistical validation of regression models. The optimum conditions for maximum rejection efficiency of 96.65% has been figured out experimentally by gradient method and was found to be as follows: $[\text{Co}^{2+}]_0 = 65 \text{ mg/L}$, polymer/metal ratio = 5.88 and pH 6.84.

© 2009 Elsevier B.V. All rights reserved.

1. Introduction

In the last quarter of a century, the presence of heavy metal ions in the environment has received extensive attention due to increased discharge, their non-biodegradable properties, toxicity in the environment, and other adverse effects which heavy metal ions have on receiving waters [1]. Cobalt is a ferromagnetic metal that has a large application in different industrial fields such as production of corrosion-resistant alloys and super-alloys for parts in gas turbine aircraft engines, magnets and magnetic recording media, catalysts for the petroleum and chemical industries as well as pigments [2]. It is also applied in the electroplating industry because

of its appearance, hardness, and resistance to oxidation. Cobalt radioisotope Co^{60} is a radioactive substance that is used in medicine for radiotherapy, as well as in a number of industrial applications. All these applications of cobalt in industry and medicine represent the potential sources for generation of wastewater streams laden with cobalt. Although cobalt is an essential element for life in tiny amounts (central component of vitamin B_{12}), at higher levels of exposure it shows carcinogenic effects similar to nickel [2].

Thus, it is indispensable to treat metal-contaminated wastewaters prior to their discharge to the environment. Various treatment techniques for wastewater laden with heavy metals ions have been developed in the last decade both to reduce the amount of wastewater produced and to improve the quality of the treated effluent [1]. Although different treatment methods such as chemical precipitation [3,4], coagulation–flocculation [4–6], electrochemical processes [7,8], ion exchange [8,9] and sorption [10–13] can be employed to remove heavy metals from wastewaters, they have their intrinsic advantages and drawbacks in application. For instance, chemical precipitation and coagulation–flocculation as well as electrochemical treatment become ineffective particularly when metal ion concentration in the solution is low (1–100 mg/L). These processes produce large quantity of sludge to be treated. Ion

Abbreviations: ANOVA, analysis of variances; CCD, central composite design; DoE, design of experiments; MEUF, micellar-enhanced ultrafiltration; MLR, multi-linear regression method; MWCO, molecular weight-cut-off; PAUF, polymer assisted ultrafiltration; PEI, polyethyleneimine; RSM, response surface methodology; RS-model, response surface model.

* Corresponding author. Permanent address: Tudor Neculai 25, 953C-14, Iași, Romania. Tel.: +40 742176747.

E-mail addresses: cojocaru.c@yahoo.com, ccojoc@gmail.com (C. Cojocaru).

¹ Visiting scientist under the aegis of Marie Curie Action ‘Transfer of Knowledge’.

Nomenclature

a	the weight of polymer (g)
b_0, b_i, b_{ij}, b_{ij}	regression coefficients in polynomial equation
\bar{b}	$(L \times 1)$ vector of regression coefficients of response surface model
C	concentration of Co^{2+} in feed solution, $[\text{Co}^{2+}]_0$ (mg/L)
C_p	concentration of Co^{2+} in permeate flux (mg/L)
DF	degree of freedom
e	residual error
F -value	ratio of variances, computed value
h	number of independent variables
i and j	subscripts (integer variables)
J	permeate flux
k	superscript, indicating the iteration of searching in gradient method
L	number of regression coefficients within RS-model
\bar{m}	vector indicating the direction of steepest ascent of the objective function
m_i	component of the direction vector
MS	mean square
M_w	molecular weight
N	number of experimental runs in CCD
P -value	statistical estimator
R^2	coefficient of multiple determination
R^2_{adj}	adjusted statistic coefficient
r	ratio of polymer (PEI) to cobalt (Co^{2+}) (w/w)
SS	sum of squares
s	integer number for adjusting the step-length in gradient method
t	time
u	number of design variables
\bar{X}	$(N \times L)$ design matrix of the independent variables levels
\bar{x}_S	vector of stationary point coordinates in coded terms
$\bar{x}^{(k)}$	vector of design variables in coded terms
x_1, x_2, x_3	coded levels of the factors (design variables)
\bar{Y}	$(N \times 1)$ vector of the experimental observations (rejection efficiency)
Y	rejection efficiency (experimental value);
\hat{Y}	rejection efficiency (predicted value by RS-model);
z_1, z_2	actual variables
*	superscript indicating optimal values of variables;

Greek letters

α	axial point or "star" point in CCD;
λ	step-length of searching in gradient method
$\omega_1, \omega_2, \omega_3$	canonical axes with origin in stationary point
Ω	valid region (initial region of experimentation)

exchange and activated carbon sorption processes are extremely expensive, especially when treating a large amount of wastewater containing low heavy metal concentration. As regards the low-cost sorbents, it should be pointed out that despite their properties of being inexpensive and easily available they have relatively low binding capacity [13]. Therefore nowadays there is a growing interest in developing and optimization of the alternative and promising methods for the removal of heavy metals from wastewaters. In this respect, the membrane enhanced ultrafiltration assisted by complexation using different water-soluble polymers has received a considerable attention for the treatment of inorganic effluent, since

it is capable of efficient treatment of different wastewaters streams laden with heavy metals ions and radionuclides [14–28].

Polymer assisted ultrafiltration (PAUF) is a hybrid process that combines two phenomena, i.e. binding of metal ions to a water-soluble polymer (complexation) and ultrafiltration. Since the pore sizes of ultrafiltration membranes are not appropriate to separate heavy metal ions, the chelating agents are used for binding the metals and to form macromolecular complexes [26–28]. These complex molecules, having a higher molecular weight than the molecular-weight-cut-off (MWCO) of the membrane, will be retained, while the non-complexed ions pass through the membrane. By means of PAUF method and using different water-soluble polymers it is possible to achieve selective separation and recovery of heavy metals with low energy requirements [26]. Highly purified permeates have been achieved using PAUF method [14–29]. Generally, the results regarding polymer assisted ultrafiltration were reported for different wastewater streams containing various species of heavy metals (Cu, Zn, Cd, Co, Ni, Pb, Fe, Cr, Mn, Hg) and different water-soluble metal-binding polymers such as polyacrylic acid (PAA), polyethyleneimine (PEI), polyvinylalcohol (PVA), polyacrylic acid sodium salt (PAASS), poly(dimethylamino-co-epichlorohydrin-co-ethylene-diamine) (PDEHED) and so forth [14–28]. The progress in macromolecular chemistry such as the invention of dendritic polymers is providing novel opportunities to develop the efficient nanoscale chelating agents for environmental and industrial applications [29]. The results presented in the reference [29] indicate that the dendrimer-enhanced ultrafiltration (DEUF) is a promising process for removal and recovery of metal ions from aqueous solutions. Another option of enhanced ultrafiltration to remove efficiently heavy metals from wastewaters deals with micellar-enhanced ultrafiltration (MEUF). This separation technique involves the addition of surfactants to contaminated aqueous solution [30–35].

Recently, the design of experiments (DoE) and response surface methodology (RSM) has been proved to be effective tools for investigation, modeling and optimization of the enhanced ultrafiltration processes. In our previous work [25] we have applied the experimental design and RSM for the optimization of hybrid complexation-ultrafiltration process for copper removal from aqueous solutions taking into account the feed concentration of polyacrylic acid (i.e. chelating agent), the pH value and the polymer to metal ratio. A good conformity was observed between the predicted and the experimental optimal conditions of polymer assisted ultrafiltration. Xiarchos et al. [35], has applied response surface methodology for the modeling of copper removal from aqueous solutions using micellar-enhanced ultrafiltration. Also, Aydiner et al. [36] applied the Taguchi experimental design to investigate the influence of factors upon on nickel rejection, surfactant rejection and steady-state flux in a surfactant-added powdered activated carbon/microfiltration hybrid process.

The present work deals with application of DoE and RSM tools for modeling and optimization of cobalt removal from aqueous solution using polymer assisted ultrafiltration process and PEI as chelating agent. The task of dead-end ultrafiltration experiments was to optimize the complexation conditions in order to ensure the maximum rejection efficiency. The optimum conditions will be applied in real ultrafiltration systems operated in cross-flow mode.

2. Materials and methods

2.1. Chemicals

All the chemicals used in experiments were of analytical reagent grade. As a source of cobalt ions, cobalt (II) chloride hexahydrate $\text{CoCl}_2 \cdot 6\text{H}_2\text{O}$ (puriss) ($M_w = 237.93$ g/mol) provided

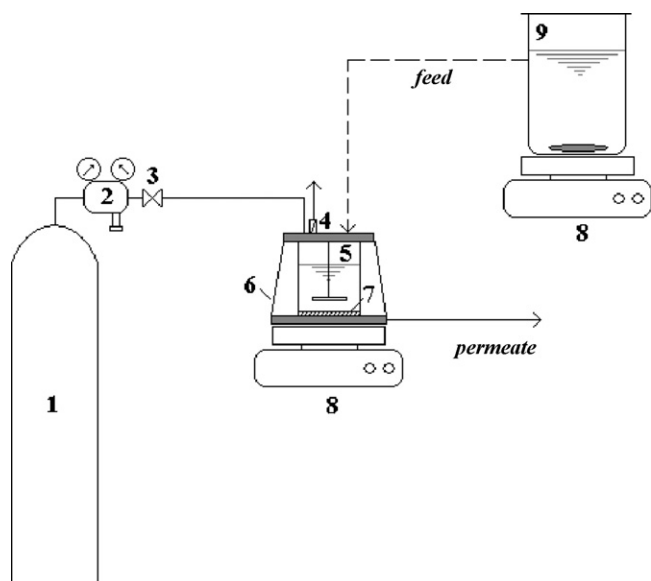


Fig. 1. Schematic diagram of batch complexation and dead-end ultrafiltration assembly. 1—Cylinder with compressed air (pressure trap); 2—reducer with diaphragm valve and pressure gauge; 3—open–close valve; 4—release valve; 5—UF stirred cell; 6—wrap-around clamp; 7—membrane; 8—magnetic stirrer and 9—batch stirred tank for complexation reaction (preparation of feed solution).

by Sigma–Aldrich was used for preparing of aqueous solutions. Polyethyleneimine of 50 wt.% solution in water with average molecular weight of $M_w = 750,000$ g/mol from Sigma–Aldrich was applied in polymer assisted ultrafiltration experiments as chelating agent. Solutions of hydrochloric acid and sodium hydroxide of 0.1 M and 0.01 M concentrations have been used for pH adjustment. Distilled water has been used in all experiments.

2.2. Analytical methods

The concentrations of cobalt ions in feed and permeate solutions were measured by an analytical kit (HACH Permachem Reagents). This method is based on a measurement of color intensity (absorbance reading at a 620 nm wavelength) of the complex formed by the reaction of cobalt with 1-(2-pyridylazo)-2-naphtol and surfactants in aqueous solution [37]. The reproducibility of the concentration measurement was within a maximum deviation of 4% in all cases studied. By means of direct reading spectrophotometer UV–vis (HACH DR/2000) the absorbance was recorded. A pH meter (OAKTON pH/CON 510) with a combined glass electrode was used for pH measurements of solution throughout the study.

2.3. Batch complexation and dead-end PAUF experiments

The schematic diagram of batch complexation and dead-end ultrafiltration assembly is shown in Fig. 1. All complexation experiments of Co (II) ions with PEI were carried out in a batch stirred tank with an initial volume of 500 mL. The chelating agent (PEI) was added to the feed solution before filtration and pH was fixed on the required level. The feed solution was gently stirred in order to achieve the equilibrium state for complexation. The operating temperature was the room temperature of 25 ± 2 °C. After the complexation reaction 35 mL of feed solution was transferred from the tank (9) into dead-end UF stirred cell (5), capacity of 50 mL (Amicon 8050 Millipore, USA). This volume transfer is indicated by discontinuous line in Fig. 1. In the UF cell a flat-sheet membrane made from regenerated cellulose and provided by Millipore (USA) was used. The commercial membrane had $MWCO = 5000$ g/mol; diameter of 4.45 cm and effective membrane area of 13.4 cm^2 . The permeate

flux of pure water in Amicon UF cell with regenerated cellulose membrane was equal $50 \text{ L/m}^2 \text{ h}$.

It should be pointed out that the dense membrane of low-cut-off (5000 g/mol) was used in these experiments to ensure the removal of the complexes formed. The feed solution in UF cell was gently stirred with magnetic stirrer to reduce concentration polarization phenomena. All experiments were carried out applying an operating pressure of 350 kPa. The rejection efficiency (noted by $Y\%$) was determined for polymer assisted ultrafiltration experiments as follows:

$$Y = \left(1 - \frac{C_p}{C}\right) \times 100 \quad (1)$$

where: C is the concentration of Co^{2+} in feed solution (mg/L) and C_p —the concentration of Co^{2+} in permeate flux (mg/L). In addition, the binding capacity q (mg/g) was ascertained from the mass balance using the subsequent equation:

$$q = \left(\frac{C - C_p}{a/1000}\right) V \quad (2)$$

where q is the binding capacity that indicates the quantity of metal uptake by polymer ($\text{mg}[\text{Co}^{2+}]/\text{g}[\text{PEI}]$), V is the volume of solution (mL) and a is the weight of polymer added (g).

3. Results and discussion

3.1. Design of experiments and response surface modeling

The water-soluble polymer PEI is a strong chelating agent with imine groups, having the following formula: $(-\text{NHCH}_2\text{CH}_2)_n[-\text{N}(\text{CH}_2\text{CH}_2\text{NH}_2)\text{CH}_2\text{CH}_2-]_y$. The donor–acceptor bonds formed between the metal and imine groups of the polymer result in complexation of cobalt with PEI. The structure of PEI–Co complex may be presented as it is shown in Fig. 2 [38]. Optimization of the significant factors in the hybrid complexation–ultrafiltration process via the conventional method of investigation involves the changing of one variable in time while all other variables are fixed at constant levels, and studying the effect of the single variable on the response. This classical approach is time-consuming and complicated for a multi-variable system. In order to overcome such difficulty, the statistical techniques as DoE and RSM for the study of PAUF process have been applied. The DoE and RSM tools are the collection of statistical and mathematical techniques used for developing, improving, and optimizing any process or experiment under study [40,44].

The experimental design used for the modeling of hybrid complexation–ultrafiltration process was carried out choosing three factors (design variables), namely: feed concentration of cobalt ions (C , mg/L), ratio of polymer (PEI) to cobalt (r , w/w) and

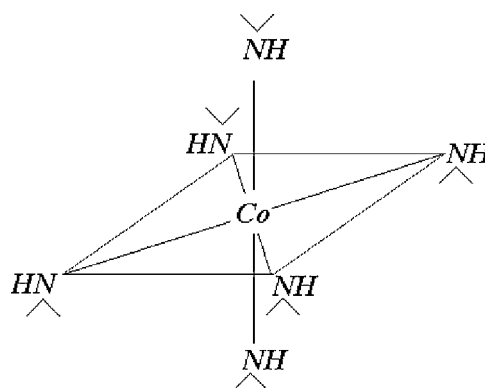


Fig. 2. Structure of Co–PEI complex.

Table 1
Design variables and their coded and actual values used for experimental design.

Design variable (factors)	Symbol	Actual values of coded levels				
		$-\alpha$	-1	0	$+1$	$+\alpha^a$
Initial concentration of cobalt in aqueous solution, $[\text{Co}^{2+}]_0$ (mg/L)	x_1	35.7	40	60	80	84.3
Ratio: PEI/cobalt, r	x_2	0.6	1	3	5	5.4
pH of solution	x_3	3.7	4.0	5.2	6.4	6.7

^a $\alpha = 1.215$ (star or axial point for orthogonal CCD in the case of 3 independent variables).

pH of feed solution. The operating ranges and the levels of the considered variables are given in actual and coded values in Table 1. A central composite design (CCD) of orthogonal type was employed in this study for planning the experiments as it is shown in Table 2. The CCD consists of three distinct sectors: (1) full factorial design in which the factor levels are coded to the usual low (-1) and high ($+1$) values; (2) axial points localized on the axis of each variable at a distance α from the designed center; and (3) center points that can be replicated to provide an estimation of the experimental error variance. The results of two responses, i.e. (1) rejection efficiency Y (%) and (2) binding capacity q (mg/g) were determined experimentally according to designed runs in order to ascertain the performance of the complexation process.

Generally, a second-order polynomial model with main, quadratic and interaction terms can be developed to fit the experimental data obtained from the experimental runs conducted on the basis of CCD. The response surface model (RS-model), known also as regression or empirical equation, represents an approximation of experimental data and is stated by the following relationship:

$$\hat{Y} = b_0 + \sum_{i=1}^u b_i x_i + \sum_{i=1}^u b_{ii} x_i^2 + \sum_{i < j}^u b_{ij} x_i x_j \quad (3)$$

where \hat{Y} denotes the predicted response (predicted rejection efficiency), x_i refers to the coded levels of the design variables, b_0 , b_i , b_{ii} , b_{ij} are the regression coefficients (offset term, main, quadratic and interaction effects) and u is the number of design variables. The least square estimations of the regression coefficients have been computed by means of multiple linear regression (MLR) method

Table 2
Central composite orthogonal design and experimental responses.

Run number (N) and type ^a	Factors (controllable input variables)							Responses	
	Initial cobalt concentration		Ratio: PEI/Co ²⁺		Initial pH of solution		Rejection efficiency	Binding capacity	
	$[\text{Co}^{2+}]_0$ (mg/L)	Level ^b x_1	r	Level ^b x_2	pH	Level ^b x_3			Y (%)
1	O1	80	1	5	1	6.4	1	93.94	193.38
2	O2	40	-1	5	1	6.4	1	87.79	179.75
3	O3	80	1	1	-1	6.4	1	21.08	221.81
4	O4	40	-1	1	-1	6.4	1	20.67	216.13
5	O5	80	1	5	1	4.0	-1	51.65	106.93
6	O6	40	-1	5	1	4.0	-1	59.34	122.85
7	O7	80	1	1	-1	4.0	-1	15.93	164.94
8	O8	40	-1	1	-1	4.0	-1	14.24	149.00
9	S1	84.3	α	3	0	5.2	0	54.17	187.11
10	S2	35.7	$-\alpha$	3	0	5.2	0	53.09	182.73
11	S3	60	0	5.4	α	5.2	0	90.15	166.19
12	S4	60	0	0.6	$-\alpha$	5.2	0	16.91	305.99
13	S5	60	0	3	0	6.7	α	66.31	229.64
14	S6	60	0	3	0	3.7	$-\alpha$	40.00	136.50
15	C1	60	0	3	0	5.2	0	53.28	184.50
16	C2	60	0	3	0	5.2	0	52.84	182.30

^a O = orthogonal design points. C = center points. S = star or axial points.

^b -1 = low value. 0 = center value. $+1$ = high value. $\pm\alpha$ = star point value.

and can be written as follows [39–41]:

$$\bar{b} = (\bar{X}^T \bar{X})^{-1} \bar{X}^T \bar{Y} \quad (4)$$

where \bar{b} is a $(L \times 1)$ vector of regression coefficients, \bar{X} is a $(N \times L)$ extended design matrix of the coded levels of input variables, \bar{Y} is a $(N \times 1)$ column vector of response determined experimentally according to the arrangement points into CCD, N is the number of experimental runs and L is the number of regression coefficients within the extended RS-model.

Based on experimental results obtained according to experimental design (Table 2) the RS-models have been constructed by MLR-method to figure out the functional relationship for approximation and prediction of rejection efficiency and binding capacity. Thus, the second-order RS-models with coded variables are as follows:

$$\hat{Y} = 57.686 + 28.285x_2 + 10.435x_3 - 3.727x_1^2 - 3.795x_2^2 - 4.049x_3^2 + 1.57x_1x_3 + 7.395x_2x_3 \quad (5)$$

$$\hat{q} = 211.648 - 29.11x_2 + 34.742x_3 - 24.15x_1^2 + 10.542x_2^2 - 25.404x_3^2$$

subjected to : $x_i \in \Omega$; $\Omega = \{x_i | -\alpha \leq x_i \leq +\alpha\}$; $\forall i=1, 3$ (6)

Note that, the term Ω means the valid region (region of experimentation) where the RS-models are valid. The significance of regression coefficients in RS-models with coded variables was tested using the statistical Student's t -test. Thus, in Eqs. (5) and (6) only significant terms were retained. The significance of RS-models was tested by means of analysis of variance (ANOVA). In this respect the F -value was determined, which is a measure of the variance of data about the mean, based on the ratio of the mean square of group variance due to error [40]. If the F -value departs significantly from unity, then it is more certain that the design variables adequately explain the variation in the mean of the data. Having the F -value and the degree of freedoms, the P -value is then calculated. If the P -value is low, one may conclude that the RS-model is statistically validated for prediction of the response. Most investigators accept the RS-model for prediction if the P -value is less than 0.05. In Tables 3 and 4 the ANOVA results are presented for both RS-models developed. The ANOVA tables summarise the sum of

Table 3
Analysis of variance (ANOVA) for RS-model (response: rejection efficiency).

Source	DF ^a	SS ^b	MS ^c	F-value	P-value	R ²	R ² _{adj}
Model	7	10595.822	1513.689	117.322	<0.0001	0.9903	0.9819
Residual	8	103.216	12.902				
Total	15	10699.038					

^a Degree of freedom.

^b Sum of squares.

^c Mean square.

Table 4
Analysis of variance (ANOVA) for RS-model (response: binding capacity).

Source	DF	SS	MS	F-value	P-value	R ²	R ² _{adj}
Model	5	27496.99	5499.39	9.343	0.0016	0.824	0.736
Residual	10	5885.85	588.585				
Total	15	33382.84					

squares of residuals and regressions together with the corresponding degrees of freedom, *F*-value, *P*-value and ANOVA coefficients (i.e. coefficients of multiple determination *R*² and adjusted statistic *R*²_{adj}). The mathematical equations used for calculation of the ANOVA estimators (i.e. SS, MS, *F*-value, *R*², *R*²_{adj}) are widely presented in the literature concerning DoE and RSM [39–41]. According to the ANOVA results focused in Table 3, the *F*-value is very high and the *P*-value is smaller than 0.0001. In addition, the *R*² value for rejection efficiency is 0.9903, close to 1, which is desirable, and the predicted *R*² is in agreement with the adjusted coefficient of determination *R*²_{adj}. All these statistical estimators reveal that the RS-model developed for the prediction of rejection efficiency is statistically validated for the approximation of the response over the range of experimentation considered (valid region). As regards the second RS-model, that set the functional relationship between

the experimental and predicted response ($e = Y_{\text{exp}} - \hat{Y}_{\text{predic}}$). The goodness-of-fit of RS-models are illustrated in Figs. 3 and 4. As one can see, both RS-models give good predictions for the investigated responses. In addition the average relative error in percentage was determined for both models. The average relative errors of 5.87 and 8.14% were obtained for predictors of rejection efficiency and binding capacity, respectively. Thus, the obtained average relative errors were lower than 10% for both RS-models considered.

For the graphical representation and response surface analysis it is worth converting the RS-models in terms of coded variables to empirical models in terms of actual variables. Hence, the empirical models in terms of actual variables may be written as:

$$\hat{Y} = -79.56 + 0.778C + 3.81r + 24.77\text{pH} - 0.0093C^2 - 0.949r^2 - 2.812\text{pH}^2 + 0.0654C \text{ pH} + 3.081r \text{ pH} \quad (7)$$

$$\hat{q} = -565.87 + 7.245C - 30.365r + 212.394\text{pH} - 0.06C^2 + 2.635r^2 - 17.639\text{pH}^2 \quad (8)$$

subjected to : $35.7 \leq C \leq 84.3$ (mg L⁻¹); $0.6 \leq r \leq 5.4$; $3.7 \leq \text{pH} \leq 6.7$;

binding capacity and factors, the ANOVA results are given in Table 4. In this case, the *F*-value is also clearly departing from unity and *P*-value is about 0.0016. The coefficient of determination for binding capacity response model is about 0.824. Thus, the statistical results from Table 4 indicate that the second RS-model is significant and may be used for the prediction as well. Likewise, the model adequacy can easily be investigated by examination of the residuals, which may be defined for any observation as the difference between

The empirical coefficients from Eqs. (7) and (8) were computed by substitution, being dependent on the values of the regression coefficients from Eqs. (5) and (6) and the operating range of each design variable.

In the next figures (Figs. 5–10) the response surfaces plots and contour-lines maps are presented for both response functions revealing the influence of factors (design variables) upon the investigated responses, i.e. rejection efficiency and binding capacity. Thus, the response surfaces illustrated in Figs. 5–7 for rejection

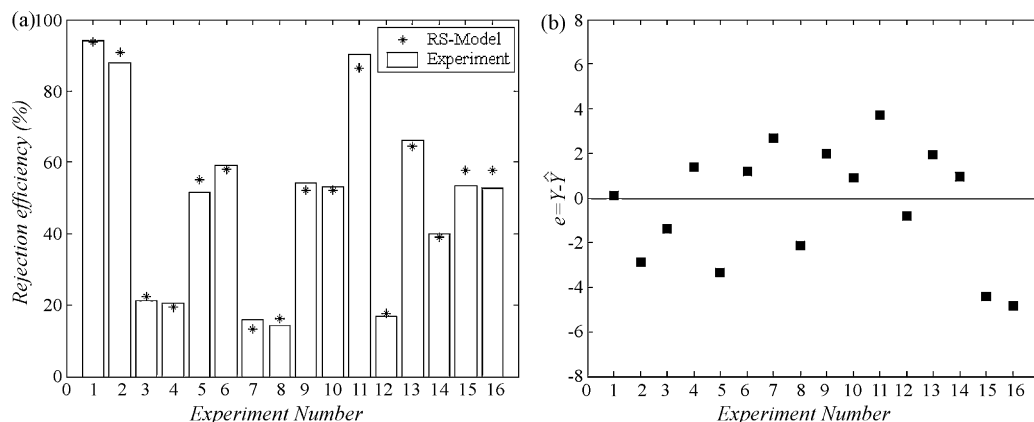


Fig. 3. Experimental data plotted against the predicted ones for rejection efficiency (a) and residuals versus observation order (b).

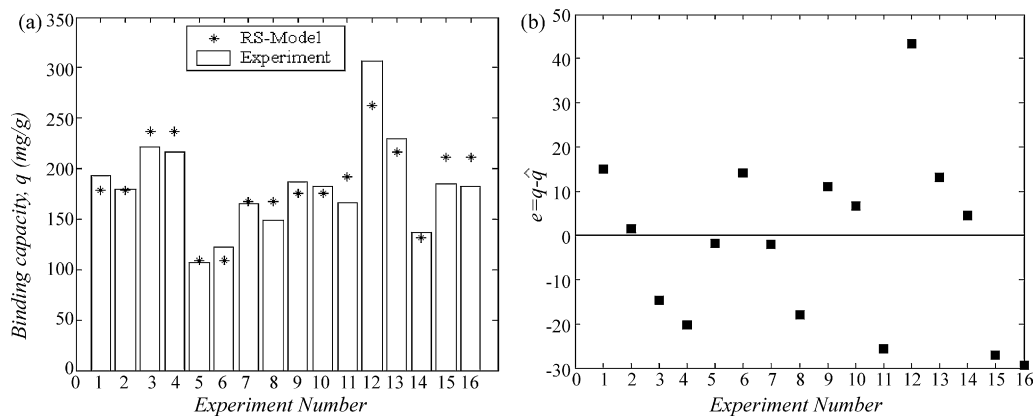


Fig. 4. Experimental data plotted against the predicted ones for binding capacity (a) and residuals versus observation order (b).

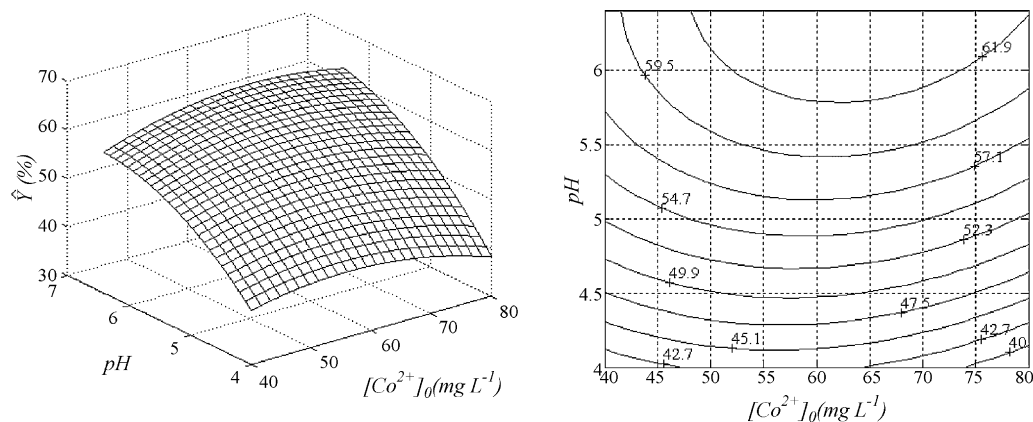


Fig. 5. \hat{Y} -response surface plot and contour-lines map depending on $[Co^{2+}]_0$ and pH variables, holding the other variable at its center level, $r=3$.

efficiency (Y -response) indicates that the increasing of both pH and polymer/metal ratio will lead to enhancing of rejection efficiency. For the third factor (i.e. initial cobalt concentration in feed solution) an optimal region where Y -response remains at maximal level can be seen in the range of 55–70 mg/L. The main effect of initial cobalt concentration factor is negligible (Figs. 5 and 6), while the polymer/metal ratio factor has the highest main effect (Figs. 6 and 7) followed by the main effect of pH factor (Fig. 7). The quadratic effects are similar for all factors giving the contribution to the response surface curvature. The small interaction effect between cobalt concentration C and pH factors can be detected from Fig. 5 and there are no interaction effects between C and r factors

(Fig. 6). In addition, the relatively strong interaction effect between r and pH variables can be seen from Fig. 7. For instance, the effect of pH variable on rejection efficiency becomes more important at higher values of polymer/metal ratio while the effect of r variable is more intense at higher pH values (Fig. 7).

The Figs. 8–10 depict the q -response surface in terms of main, interaction and quadratic effects of design variables (factors). The response surface analysis in this case indicates that the increment of pH up to value 5.5 leads to increasing of binding capacity q ; after that (i.e. in the interval 5.5–6.7 pH) the elliptical contour-lines indicate the existence of optimal pH region that maximizes the binding capacity. The increase in the initial cobalt concentration up

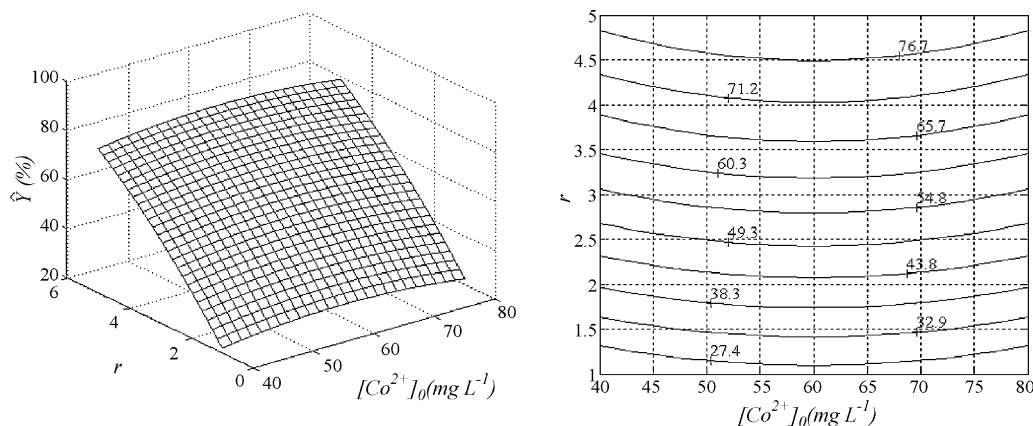


Fig. 6. \hat{Y} -response surface plot and contour-lines map depending on $[Co^{2+}]_0$ and r variables, holding the other variable at its center level, pH 5.2.

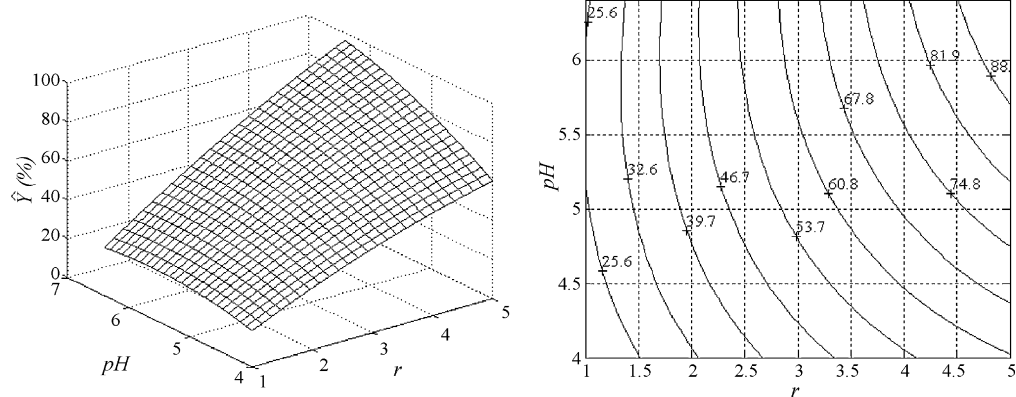


Fig. 7. \hat{Y} -response surface plot and contour-lines map depending on pH and r variables, holding the other variable at its center level, $[\text{Co}^{2+}]_0 = 60$ (mg/L).

to 55 mg/L enhances the q -response function. For the concentration interval 55–65 mg/L the variation of binding capacity is not significant and q -response remains at superior levels. For higher value of initial metal concentration (i.e. >65 mg/L) the binding capacity has the trend of decreasing. Concerning the polymer/metal ratio factor, the growth of this variable lead to decrease in binding capacity. So that, at the lower values of polymer/metal ratio the binding capacity will be the highest. This can be attributed to different equilibrium states at lower and higher values of polymer dosage. Thus, at the lowest PEI dosage the polymer will be almost completely “consumed” for binding the metal ions that are in surplus state comparing with polymer amount. The binding capacity in this case will be the highest one. With the increasing of polymer dosage (polymer/metal ratio) the changes in equilibrium state leads

to diminishing of binding capacity. The main effect of C factor on binding capacity is negligible (Figs. 8 and 10) while the highest main effect upon binding capacity is attributed to pH followed by r factor (Fig. 9). The quadratic effects appear for all factors while the interaction effects between them are non-significant.

3.2. Canonical analysis and response surface optimization

Since the batch complexation and dead-end PAUF experiments were devoted for determination of optimal conditions of complexation reaction to ensure the maximal retention of the complexes by the membrane, the response of primary importance was the rejection efficiency. Therefore, for the optimization issue the Y -response equation was selected as objective function. The canonical analysis

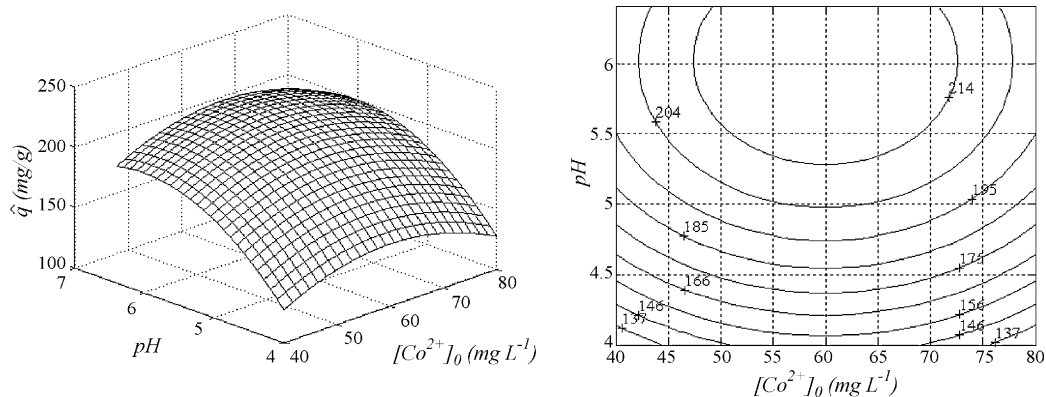


Fig. 8. \hat{q} -response surface plot and contour-lines map depending on $[\text{Co}^{2+}]_0$ and pH variables, holding the other variable at its center level, $r = 3$.

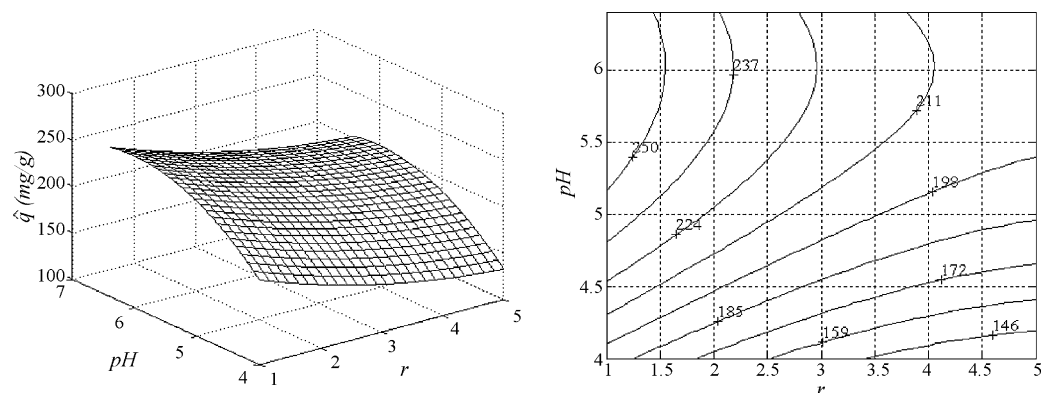


Fig. 9. \hat{q} -response surface plot and contour-lines map depending on pH and r variables, holding the other variable at its center level, $[\text{Co}^{2+}]_0 = 60$ (mg/L).

Table 5
The feasible optimal point for complexation process (Co-PEI) determined by stochastic simulations (experimental value vs. predicted one).

Initial concentration of Co^{2+} in aqueous solution		Ratio: PEI/ Co^{2+}		pH of solution		Y.(%) experiment	Y.(%) RS-model
x_1	$[\text{Co}^{2+}]_0$ (mg/L)	x_2	r	x_3	pH		
0.241	65	1.215	5.4	1.215	6.7	95.28	104.30

was employed to figure out the stationary point and its nature. In our case the canonical form of Y-response model becomes as follows:

$$\hat{Y} - \hat{Y}_S = -3.73\omega_1^2 - 0.138\omega_2^2 - 7.703\omega_3^2 \quad (9)$$

where \hat{Y}_S means the value of response function in stationary point and ω_1 , ω_2 and ω_3 are canonical axes with origin in the stationary point. Since the canonical coefficients have negative signs the stationary point is a maximum point. The coordinates of stationary point in terms of coded variables are $\bar{x}_S = [14.228 \ 69.54 \ 67.549]^T$ revealing that this point is located outside of the valid region and $\hat{Y}(\bar{x}_S) = \hat{Y}_S = 1.393 \times 10^3$. So that, the stationary point (absolute maximum) cannot be used as optimal solution in our problem. Therefore, for determining of feasible optimal point inside of valid region the numerical simulations were carried out. In this respect Monte-Carlo stochastic simulation method [42] was applied using a multi-stage approach and a zooming-in technique in order to determine the feasible optimal point more accurately. The results concerning feasible optimal point found are reported in Table 5.

The experimental value of response in feasible optimal point ($Y=95.28\%$) is higher than any rejection efficiency value achieved in the initial experiments conducted according to experimental design (Table 2). In addition, the value of binding capacity q was determined for feasible optimal point. Thus, the binding capacity given by approximation model in this point is about 195.09 mg/g while the experimental one is about 183.39 mg/g.

As one can see, for the feasible optimal point the both variables r and pH were converged to the boundary of valid region (region of experimentation). Therefore it was of interest to explore these variables beyond of initial region of experimentation. Since the RS-model cannot be used for the prediction beyond these limits, an additional experimental optimization approach based on gradient method was used in order to explore the r and pH factors further than initial region of experimentation. The feasible optimal point determined by response surface optimization was taken as the start point in this additional experimental approach.

3.3. Experimental optimization by gradient method

To figure out the optimal solutions by gradient methods the values of both the objective function (response function) and its first order partial derivatives should be known [43]. According to the methodology of gradient algorithms, the advance towards optimum is accomplished in gradient direction. As it is already known, the gradient of a response function $Y(\bar{z})$ in a point is the assembly of first order partial derivatives of the function of several variables in the considered point $\bar{z}^{(0)}$, that is:

$$[\text{grad } Y(\bar{z})]_{\bar{z}^{(0)}} = \left[\frac{\partial Y}{\partial z_1} \quad \frac{\partial Y}{\partial z_2} \quad \dots \quad \frac{\partial Y}{\partial z_h} \right]_{\bar{z}^{(0)}}^T \quad (10)$$

where h is the number of independent variables.

The gradient direction, as a vector, depends upon the coordinates of this point and indicates the direction of steepest descent $[-\text{grad } Y(\bar{z})]$ or steepest ascent $[\text{grad } Y(\bar{z})]$ of the objective function in the considered point.

The one step displacement $\lambda^{(k)}$ from a certain point $\bar{z}^{(k)}$ into another $\bar{z}^{(k+1)}$ is given by the subsequent equation [43]:

$$\bar{z}^{(k+1)} = \bar{z}^{(k)} + \bar{m}^{(k)}\lambda^{(k)} \quad (11)$$

or in terms of components:

$$z_i^{(k+1)} = z_i^{(k)} + m_i^{(k)}\lambda^{(k)} \quad \forall i = 1, 2, \dots, h \quad (12)$$

where the directions of steepest ascent/descent are given by following equation:

$$m_i^{(k)} = \frac{\pm(\partial Y/\partial z_i)_{\bar{z}^{(k)}}}{\sqrt{\sum_{i=1}^h (\partial Y/\partial z_i)^2}} \quad (13)$$

In the above relationship the signs (+) and (–) correspond to maximizing and minimizing issue, respectively. If the mathematical expression of the objective function (response function) is not known for a specific region of experimentation, but the experimental system for optimization is available, one can proceed as follows.

- 1) A start point is chosen $\bar{z}^{(0)}$ and the gradient components in the considered point are determined experimentally. For instance, if for unknown explicit relationship $Y=f(z_1, z_2)$, the variable z_1 is increased by $\Delta z_1^{(0)}$ when keeping z_2 at constant level, and then

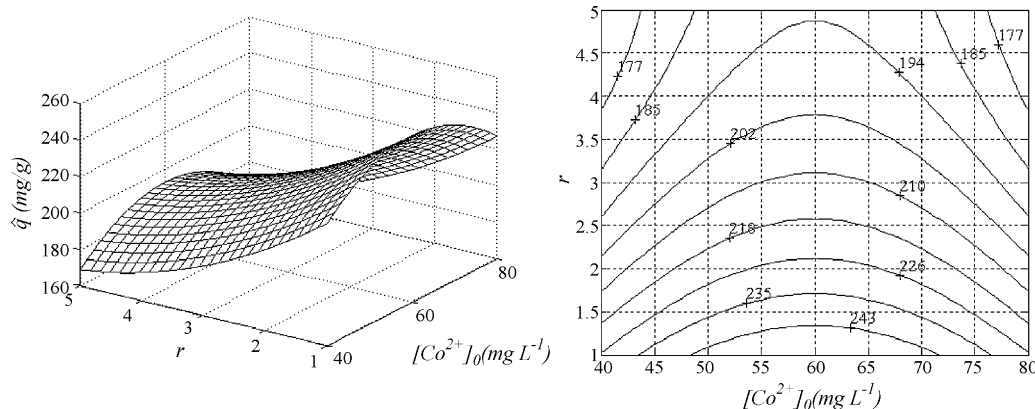


Fig. 10. \hat{q} -response surface plot and contour-lines map depending on $[\text{Co}^{2+}]_0$ and r variables, holding the other variable at its center level, pH 5.2.

Table 6

Experimental design carried out according to the gradient method, $[\text{Co}^{2+}]_0 = 65 \text{ mg/L}$ (for each run).

No.	z_1 (polymer/metal ratio)	z_2 (pH)	Y (%) rejection efficiency (experimental values)
1	5.4	6.7	95.28
2	6.2	6.7	96.18
3	5.4	8.4	95.83

the variable z_2 is increment by $\Delta z_2^{(0)}$ when keeping z_2 constant, the corresponding values of Y-response should be measured every time. Let $\Delta Y_1^{(0)}$ and $\Delta Y_2^{(0)}$ be the experimentally determined increases of the Y-response in this case. These increments can be considered as proportional to the partial derivatives in the considered start point $\bar{z}^{(0)}$, that is:

$$\left(\frac{\partial Y}{\partial z_1}\right)_{\bar{z}^{(0)}} \cong \left(\frac{\Delta Y_1^{(0)}}{\Delta z_1^{(0)}}\right) \quad (14)$$

$$\left(\frac{\partial Y}{\partial z_2}\right)_{\bar{z}^{(0)}} \cong \left(\frac{\Delta Y_2^{(0)}}{\Delta z_2^{(0)}}\right) \quad (15)$$

and the gradient in this case can be written as following:

$$[\text{grad } Y(\bar{z}^{(0)})] \cong \left[\frac{\Delta Y_1^{(0)}}{\Delta z_1^{(0)}}, \frac{\Delta Y_2^{(0)}}{\Delta z_2^{(0)}} \right]^T \quad (16)$$

- 2) The directions of steepest ascent/descent, i.e. m_1^0 and m_2^0 , respectively are calculated by means of Eq. (13).
- 3) A fixed length-step, namely, λ , is chosen and the coordinates of new point $\bar{z}^{(1)} = [z_1^{(1)} \ z_2^{(1)}]^T$ are computed according to Eq. (11) and the response $Y(\bar{z}^{(1)})$ is determined experimentally.
- 4) The calculations could be repeated starting from new point $\bar{z}^{(1)}$. Thus, the components of gradient in this point are experimentally determined, as for point $\bar{z}^{(0)}$ and so on.

The above-described gradient method was applied as additional approach to response surface optimization in order to determine the best conditions of complexation beyond of initial region of experimentation where the RS-model is not confirmed and cannot be used for the prediction. In this experimental approach (gradient method) only two variables from three were selected for optimization. These variables are z_1 —the polymer/metal ratio (r) and z_2 —pH of solution. The third variable, i.e. initial concentration of cobalt was fixed at constant level (optimal value) in all experiments concerning gradient method, i.e. $[\text{Co}^{2+}]_0 = 65 \text{ mg/L}$. This factor (initial cobalt concentration) was kept constant since it did not converge to the border of valid region as others in the response surface optimization approach. Thus, the experimental optimization by gradient method was reduced to the two-variable problem.

The experimental design carried out according to gradient method is shown in Table 6. The value of rejection or removal efficiency Y in each test was determined experimentally.

The determining of gradient components and the corresponding steepest ascent directions based on experimental results listed in Table 6 is discussed as follows: The start point $\bar{z}^{(0)}$ that was used has coordinates $z_1^{(0)} = 5.4$ and $z_2^{(0)} = 6.7$, respectively. Under these conditions the rejection efficiency obtained was of 95.28% (run no. 1 in Table 6). In fact, the start point is identical with the feasible optimal point determined by response surface optimization. In a new test (run no. 2) the variable z_1 was modified by the increment Δz_1 when keeping z_2 constant. In this case the new experimental conditions become: $z_1 = 6.2$ and $z_2 = 6.7$, respectively and the obtained removal efficiency is 96.18% (run no. 2 in Table 6). Thus, a

Table 7

The experimental optimization of complexation conditions according to gradient method, $[\text{Co}^{2+}]_0 = 65 \text{ mg/L}$.

s	$\lambda = 0.25 \times s$	z_1 (polymer/metal ratio)	z_2 (pH)	Y (%) removal efficiency (experimental value)
1	0.25	5.64	6.77	95.79
2	0.5	5.88	6.84	96.65
3	0.75	6.12	6.91	94.84
4	1	6.36	6.98	93.98

0.9% response increase is noticed as a consequence of the modification of the variable z_1 by increment $\Delta z_1 = 0.8$. According to these results the following approximation was considered:

$$\left(\frac{\partial Y}{\partial z_1}\right)_{\bar{z}^{(0)}} \cong \left(\frac{\Delta Y_1^{(0)}}{\Delta z_1^{(0)}}\right) = \frac{0.9}{0.8} = 1.125 \quad (17)$$

Then the changing in z_2 variable was achieved by increasing it with $\Delta z_2 = 1.7$ and keeping the other variable constant, i.e. z_1 . Under the new experimental conditions the experimental value of removal efficiency was 95.83% (run no. 3 in Table 6) and the corresponding variation ΔY was 0.55%. Therefore the considered approximation may be written as:

$$\left(\frac{\partial Y}{\partial z_2}\right)_{\bar{z}^{(0)}} \cong \left(\frac{\Delta Y_2^{(0)}}{\Delta z_2^{(0)}}\right) = \frac{0.55}{1.7} = 0.324 \quad (18)$$

and the gradient in point $\bar{z}^{(0)}$ is as follows:

$$[\text{grad } Y(\bar{z}^{(0)})] \cong \left[\frac{\Delta Y_1^{(0)}}{\Delta z_1^{(0)}}, \frac{\Delta Y_2^{(0)}}{\Delta z_2^{(0)}} \right]^T = [1.125 \ 0.324]^T \quad (19)$$

Based on gradient components the directions of steepest ascent were computed according to Eq. (13), thus $m_1^0 = 0.961$ and $m_2^0 = 0.276$. The new points toward the direction of steepest ascent were calculated using Eq. (12) and four different values of step-length λ as is shown in Table 7. The distinctive step-lengths were calculated as $\lambda = 0.25 \times s$ where s denotes an integer number for adjusting the best step-length toward the directions of steepest ascent.

As one can see from Table 7, the maximum removal efficiency of $Y = 96.65\%$ was obtained for $z_1 = 5.88$ and $z_2 = 6.84$ by using an optimal length-step of $\lambda = 0.5$ towards the direction of steepest ascent (i.e. $\bar{m}^{(0)} = [0.961 \ 0.276]^T$).

The optimal conditions of complexation determined by gradient method (experimental optimization approach) are as follows: $[\text{Co}^{2+}]_0 = 65 \text{ mg/L}$, $r = 5.88$ and pH 6.84 in such conditions the rejection efficiency of 96.65% was obtained. This value ($Y = 96.65\%$) is the highest rejection efficiency value obtained in all experiments conducted in this work concerning the complexation of Co^{2+} with PEI followed by ultrafiltration on regenerated cellulose membrane. It is worth noting that there is a difference between the removal efficiency value (96.65%) obtained by gradient method and that obtained by response surface optimization (95.28%). This difference is due to the accuracy by which the RS-model describes the dependence between response (rejection efficiency) and the design variables, on one hand, and to the limitation of the initial experimental range where the RS-model is valid over, on the other hand. As one can see, both the optimum ratio between polymer and metal as well as the optimum value of pH of solution established by gradient method exceed the initial experimental range given by CCD for which the response surface equation (RS-model) is valid over.

Additionally, a set of experiments was carried out for optimal conditions of complexation in order to figure out the evolution of permeate flux as well the average permeate flux (Fig. 11). The regression analysis was employed to fit the experimental results. Thus, the permeate flux J (experimental data) was fitted well by the

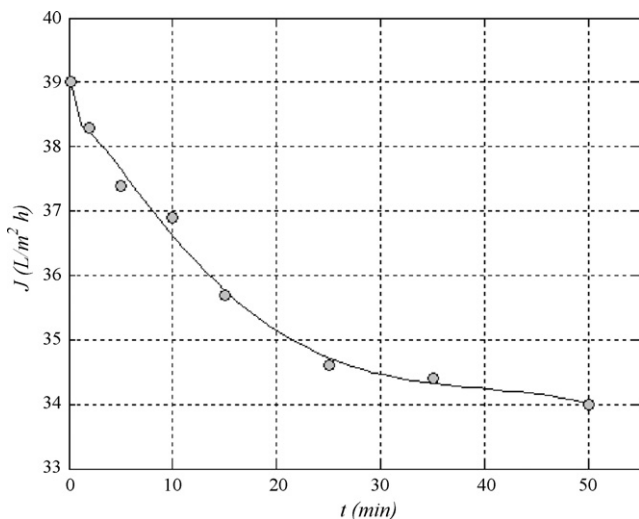


Fig. 11. Permeate flux vs. time for dead-end polymer assisted ultrafiltration system. Membrane: regenerated cellulose (5 kDa), $[\text{Co}^{2+}]_0 = 65 \text{ mg/L}$, $r = 5.88$ and pH 6.84. Solid lines: prediction given by regression model.

following non-linear regression equation:

$$J = 37.49 + 1.228\sqrt{t} - 0.58t + 0.216t^{-1} + 0.011t^2 - 8.757 \times 10^{-5}t^3 \quad (20)$$

where t means time (min). The goodness-of-fit was assigned by means of average relative error which was about 0.3%. The average permeate flux was determined by integration of the regression equation (Eq. (20)) with time. The value of 34.94 ($\text{L}/\text{m}^2 \text{ h}$) was obtained for average permeate flux. Likewise the permeate flux decline was estimated from Fig. 11 being about 13%.

4. Conclusions

The statistical experimental design of CCD-type was applied for the investigation and response surface modeling of hybrid complexation-ultrafiltration process (in dead-end mode) for cobalt removal from the synthetic wastewaters using PEI as chelating agent.

The constructed RS-models were statistically validated by ANOVA and used for the prediction of rejection efficiency and binding capacity over the valid region (region of experimentation given by CCD). Also, the 3D plots as well as contour-line maps were drawn for spatial representation and analysis of the response surface functions. Based on the RS-model developed for the prediction of rejection efficiency the feasible optimum conditions established for the valid region were computed by means of multi-stage Monte-Carlo simulation technique using a zooming-in approach. In these conditions (i.e. $[\text{Co}^{2+}]_0 = 65 \text{ mg/L}$, $r = 5.4$ and pH 6.7) the experimental value of rejection efficiency of 95.28% was obtained.

The additional experimental optimization of the process according to the algorithm of the gradient method was also accomplished to explore the limits of initial region of experimentation. The optimal experimental conditions of hybrid complexation-ultrafiltration process that ensure a maximum rejection efficiency of $Y = 96.65\%$ throughout all experiments (extensive experimentation region) were determined by gradient method and are as follows: $[\text{Co}^{2+}]_0 = 65 \text{ mg/L}$, $r = 5.88$ and pH 6.84. For the optimal conditions of complexation an average permeate flux of 34.94 ($\text{L}/\text{m}^2 \text{ h}$) and a flux decline of 13% was obtained experimentally.

Acknowledgement

The authors appreciatively acknowledge the financial support of this research work from FP6 European Funds under Marie Curie project: AMERAC no. MTKD-CT-2004-509226.

References

- [1] T.A. Kurniawan, G.Y.S. Chan, W.H. Lo, S. Babel, Physico-chemical treatment techniques for wastewater laden with heavy metals, *Chem. Eng. J.* 118 (2006) 83–98.
- [2] Cobalt - from Wikipedia (the net encyclopedia), available on-line at: <http://en.wikipedia.org/wiki/Cobalt>.
- [3] O. Tunay, N.I. Kabdasi, Hydroxide precipitation of complexed metals, *Water Res.* 28 (10) (1994) 2117–2124.
- [4] L. Charentanarak, Heavy metals removal by chemical coagulation and precipitation, *Water Sci. Technol.* 39 (10/11) (1999) 135–138.
- [5] Y.J. Li, X.P. Zeng, Y.F. Liu, S.S. Yan, Z.H. Hu, Ya-Ming, Study on the treatment of copper-electroplating wastewater by chemical trapping and flocculation, *Sep. Purif. Technol.* 31 (2003) 91–95.
- [6] L. Semerjian, G.M. Ayoub, High-pH-magnesium coagulation-flocculation in wastewater treatment, *Adv. Environ. Res.* 7 (2003) 389–403.
- [7] L.J.J. Janssen, L. Koene, The role of electrochemistry and electrochemical technology in environmental protection, *Chem. Eng. J.* 85 (2002) 137–146.
- [8] A. Smara, R. Delimi, E. Chainet, J. Sandeaux, Removal of heavy metals from diluted mixtures by a hybrid ion-exchange/electrodialysis process, *Sep. Purif. Technol.* 57 (2007) 103–110.
- [9] A. Dabrowski, Z. Hubicki, P. Podkoscielny, E. Robens, Selective removal of the heavy metals from waters and industrial wastewaters by ion-exchange method, *Chemosphere* 56 (2) (2004) 91–106.
- [10] R. Leyva-Ramos, L.A.B. Jacome, J.M. Barron, L.F. Rubio, R.M.G. Coronado, Adsorption of zinc(II) from an aqueous solution onto activated carbon, *J. Hazard. Mater.* B90 (2002) 27–38.
- [11] L. Monser, N. Adhoum, Modified activated carbon for the removal of copper, zinc, chromium, and cyanide from wastewater, *Sep. Purif. Technol.* 26 (2002) 137–146.
- [12] K.F. Lam, K.L. Yeung, G. McKay, Efficient Approach for Cd^{2+} and Ni^{2+} removal and recovery using mesoporous adsorbent with tunable selectivity, *Environ. Sci. Technol.* 41 (2007) 3329–3334.
- [13] S.E. Bailey, T.J. Olin, R.M. Bricka, D.D. Adrian, A review of potentially low-cost sorbents for heavy metals, *Water Res.* 33 (11) (1999) 2469–2479.
- [14] R. Molinari, P. Argurio, T. Poerio, Comparison of PEI, PAA and PDEHED in Cu^{2+} removal from wastewaters by PAUF, *Desalination* 162 (2004) 217–228.
- [15] R. Molinari, S. Gallo, P. Argurio, Metal ions removal from wastewater or washing water from contaminated soil by ultrafiltration-complexation, *Water Res.* 38 (3) (2004) 593–600.
- [16] M. Vieira, C.R. Tavares, R. Bergamasco, J.C.C. Petrus, Application of ultrafiltration-complexation process for metal removal from pulp and paper industry wastewater, *J. Membr. Sci.* 194 (2) (2001) 273–276.
- [17] C.R. Tavares, M. Vieira, J.C.C. Petrus, E.C. Bortoletto, F. Ceravollo, Ultrafiltration-complexation process for metal removal from pulp and paper industry wastewater, *Desalination* 144 (1–3) (2002) 261–265.
- [18] J. Barron-Zambrano, S. Laborie, Ph. Viers, M. Rakib, G. Durand, Mercury removal from aqueous solutions by complexation-ultrafiltration, *Desalination* 144 (1–3) (2002) 201–206.
- [19] S. Petrov, V. Nenov, Removal and recovery of copper from wastewater by a complexation-ultrafiltration process, *Desalination* 162 (2004) 201–209.
- [20] S. Verbych, M. Bryk, M. Zaichenko, Water treatment by enhanced ultrafiltration, *Desalination* 198 (1–3) (2006) 295–302.
- [21] K. Trivunac, S. Stevanovic, Removal of heavy metal ions from water by complexation-assisted ultrafiltration, *Chemosphere* 64 (3) (2006) 486–491.
- [22] A. Aliane, N. Bounatiro, A.T. Cherif, D.E. Akretche, Removal of chromium from aqueous solution by complexation-ultrafiltration using a water-soluble macroligand, *Water Res.* 35 (9) (2001) 2320–2326.
- [23] G. Zakrzewska-Trznel, Radioactive solutions treatment by hybrid complexation-UF/NF process, *J. Membr. Sci.* 225 (2003) 25–39.
- [24] G. Zakrzewska-Trznel, M. Harasimowicz, Removal of radionuclides by membrane permeation combined with complexation, *Desalination* 144 (2002) 207–212.
- [25] C. Cojocaru, G. Zakrzewska-Trznel, Response surface modeling and optimization of copper removal from aqua solutions using polymer assisted ultrafiltration, *J. Membr. Sci.* 298 (2007) 56–70.
- [26] M.K. Aroua, F.M. Zuki, N.M. Sulaiman, Removal of chromium ions from aqueous solutions by polymer-enhanced ultrafiltration, *J. Hazard. Mater.* 147 (2007) 752–758.
- [27] R.S. Juang, C.H. Chiou, Ultrafiltration rejection of dissolved ions using various weakly basic water-soluble polymers, *J. Membr. Sci.* 177 (2000) 207–214.
- [28] R.S. Juang, R.C. Shiau, Metal removal from aqueous solutions using chitosan-enhanced membrane filtration, *J. Membr. Sci.* 165 (2000) 159–167.
- [29] M.S. Diallo, S. Christie, P. Waminathan, J.H. Johnson Jr., W.A. Goddard, Dendrimer enhanced ultrafiltration. 1. Recovery of $\text{Cu}(\text{II})$ from aqueous solutions using PAMAM dendrimers with ethylene diamine core and terminal NH_2 groups, *Environ. Sci. Technol.* 39 (2005) 1366–1377.

- [30] A. Witek, A. Kotuniewicz, B. Kurczewski, M. Radziejowska, M. Hatalski, Simultaneous removal of phenols and Cr^{3+} using micellar-enhanced ultrafiltration process, *Desalination* 191 (2006) 111–116.
- [31] X. Ke, Z. Guang-Ming, H. Jin-Hui, W. Jiao-Yi, F. Yao-Yao, H. Guohe, L. Jianbing, X. Beidou, L. Hongliang, Removal of Cd^{2+} from synthetic wastewater using micellar-enhanced ultrafiltration with hollow fiber membrane, *Colloids Surf. A: Physicochem. Eng. Aspects* 294 (2007) 140–146.
- [32] R.S. Juang, Y.Y. Xu, C.L. Chen, Separation and removal of metal ions from dilute solutions using micellar-enhanced ultrafiltration, *J. Membr. Sci.* 218 (2003) 257–267.
- [33] F. Ferella, M. Prisciandaro, I. Michelis, F. Veglio, Removal of heavy metals by surfactant-enhanced ultrafiltration from wastewaters, *Desalination* 207 (2007) 125–133.
- [34] S. Islamogalu, L. Yilmaz, Effect of ionic strength on the complexation of polyethyleneimine (PEI) with Cd^{2+} and Ni^{2+} in polymer enhanced ultrafiltration (PEUF), *Desalination* 200 (2006) 288–289.
- [35] I. Xiarchos, A. Jaworska, G. Zakrzewska-Trznadel, Response surface methodology for the modelling of copper removal from aqueous solutions using micellar-enhanced ultrafiltration, *J. Membr. Sci.* 321 (2008) 222–231.
- [36] C. Aydinler, M. Bayramoglu, S. Kara, B. Keskinler, O. Ince Nickel, Removal from waters using surfactant-enhanced Hybrid PAC/MF process. I. The influence of system-component variables, *Ind. Eng. Chem. Res.* 45 (2006) 3926–3933.
- [37] H. Watanabe, Spectrophotometric determination of cobalt with 1-(2-pyridylazo)-2-naphthol and surfactants, *Talanta* 21 (4) (1974) 295–302.
- [38] Q. Zhu, B. Shentu, Q. Liu, Z. Weng, Swelling behavior of polyethylenimine–cobalt complex in water, *Eur. Polym. J.* 42 (2006) 1417–1422.
- [39] G.E.P. Box, N.R. Draper, *Response Surfaces, Mixtures and Ridge Analyses*, second ed., John Wiley & Sons, New York, 2007.
- [40] D.C. Montgomery, *Design and Analysis of Experiments*, fifth ed., John Wiley & Sons, New York, 2001.
- [41] S. Akhnazarova, V. Kafarov, *Experiment Optimization in Chemistry and Chemical Engineering*, Mir Publishers, Moscow, 1982.
- [42] M. Redhe, M. Giger, L. Nilsson, An investigation of structural optimization in crashworthiness design using a stochastic approach, *Struct. Multidisc. Optim.* 27 (2004) 446–459.
- [43] M. Macoveanu, G. Juncu, R. Vasiliu, Optimization of anodic oxidation of sulfuric acid solutions, *Hung. J. Ind. Chem.* 15 (3) (1987) 277–328.
- [44] R.H. Myers, D.C. Montgomery, *Response Surface Methodology: Process and Product Optimization Using Designed Experiments*, second ed., John Wiley & Sons, New York, 2002.